

BNL – 68383

High-Gain Harmonic Generation Free-Electron Laser At Saturation

T. Shaftan, M. Babzien, I. Ben-Zvi, L.F. DiMauro, A. Doyuran, W. Graves,
E. Johnson, S. Krinsky, R. Malone, I. Pogorelsky, B. Sheehy, J. Skaritka,
L. Solomon, G. Rakowsky, J.H. Wu, X.J. Wang, M. Woodle, V. Yakimenko and L.-H. Yu
National Synchrotron Light Source
Brookhaven National Laboratory
Upton, New York, 11973-5000

S.G. Biedron, J.N. Galayda, G. Gluskin, J. Jagger, V. Sajaev and I. Vasserman
Advanced Photon Source
Argonne National Laboratory
Argonne, Illinois 60439

June 2001

National Synchrotron Light Source

Brookhaven National Laboratory
Operated by
Brookhaven Science Associates
Upton, New York 11973

Under Contract with the United States Department of Energy
Contract Number DE-AC02-98CH10886

DISCLAIMER

This report was prepared as an account of work sponsored by an agency of the United States Government. Neither the United States Government nor any agency thereof, nor any of their employees, nor any of their contractors, subcontractors or their employees, makes any warranty, express or implied, or assumes any legal liability or responsibility for the accuracy, completeness, or any third party's use or the results of such use of any information, apparatus, product, or process disclosed, or represents that its use would not infringe privately owned rights. Reference herein to any specific to any specific commercial product, process, or service by trade name, trademark, manufacturer, or otherwise, does not necessary constitute or imply its endorsement, recommendation, or favoring by the United States Government or any agency thereof or its contractors or subcontractors. The views and opinions of authors expresses herein do not necessarily state to reflect those of the United States Government or any agency thereof.

High-Gain Harmonic Generation Free-Electron Laser at Saturation

T. Shaftan^{†1}, M. Babzien¹, I. Ben-Zvi¹, S. G. Biedron², L. F. DiMauro¹, A. Doyuran¹, J.N. Galayda², E. Gluskin², W. Graves¹, J. Jagger², E. Johnson¹, S. Krinsky¹, R. Malone¹, I. Pogorelsky¹, V. Sajaev², B. Sheehy¹, J. Skaritka¹, L. Solomon¹, G. Rakowsky¹, I. Vasserman², J.H. Wu¹, X.J. Wang¹,
M. Woodle¹, V. Yakimenko¹, L.-H. Yu¹,

¹ Brookhaven National Laboratory, Upton, New York 11973

²Advanced Photon Source, Argonne National Laboratory, Argonne, Illinois 60439

Abstract

We report on observations of the output of a high-gain harmonic-generation (HGFG) free-electron laser (FEL) at saturation. A seed CO₂ laser at a wavelength of 10.6- μ m was used to generate amplified FEL output at 5.3- μ m. Measurement of the frequency spectrum, pulse duration and correlation length of the 5.3- μ m output, verified the longitudinal coherence of the light. At the exit of the device, measurements of the energy distribution of the electron beam indicated that the HGFG process had reached saturation. Comparing the intensities of the higher harmonics (2.65- μ m and 1.77- μ m) relative to the 5.3- μ m fundamental, additional evidence confirming saturated operation was obtained. These results agree with theoretical predictions at saturation.

We also briefly describe the status of a new HGFG experiment at Source Development Laboratory (BNL), aiming to achieve generation of 100 nm radiation.

1. INTRODUCTION

In the HGFG scheme [1] a coherent seed at a wavelength that is a subharmonic of the desired output radiation interacts with the electron beam in an energy-modulating section. This energy modulation is then converted into spatial bunching while traversing a dispersive section. In the second undulator (the radiator), the microbunched electron beam first emits coherent radiation and then amplifies it exponentially until saturation is achieved.

A schematic of the HGFG ATF layout [2] with electron beam, seed laser and calculated HGFG radiation parameters are shown in Fig. 1.

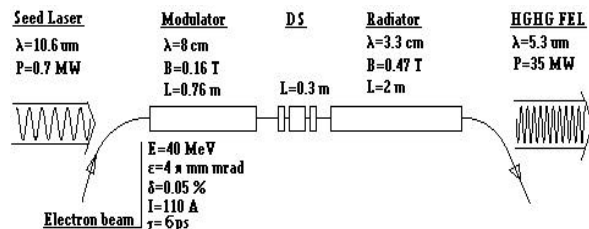


Fig. 1. HGFG ATF layout

The frequency-quadrupled Nd:YAG photocathode-rf gun drive-laser has a pulse length of 8 ps and an energy of 8 μ J resulting in a 6-ps FWHM electron beam pulse-length with a maximum of 130 A peak current off the Mg-cathode. The electron beam is accelerated via two 3-m, SLAC-type, constant-gradient, accelerating structures before being bent to enter the ATF experimental hall where it is introduced to the HGFG beamline after passage through a second dipole magnet. This bending dipole also allows an area where the CO₂ seed laser can be introduced. The seed laser delivers 4 mJ at a 10.6- μ m.

2. THE MEASUREMENTS OF HGFG RADIATION PROPERTIES

We have performed a sequence of the experiments to measure the main parameters of HGFG radiation pulse, such as frequency spectrum and coherence length, pulse length and higher harmonics content.

We used an optical spectrometer and thermal camera to measure a single-shot HGFG spectrum. The multi-shot and single-shot spectra are shown in the top and bottom figures in Figure 2, respectively.

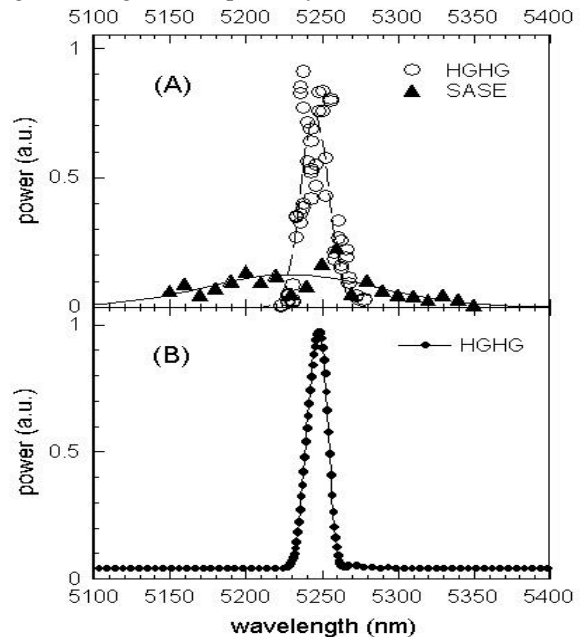


Fig. 2. The multi-shot and single-shot spectra

The top figure shows the multi-shot spectra based on the SASE signal $\times 10^6$, where every point was averaged over ten shots, as well as the HGHG signal, where no averaging was used, obtained using a high-gain, In-Sb detector. The bottom figure shows the single-shot HGHG spectrum obtained using the thermal imager described above. The resolution of this experiment is 2 nm.

For investigation of the time coherence of the HGHG radiation we have used Michelson interferometer. The mirror in one arm was tilted off-axis and changing the angle of tilt we controlled the number of periods in interference pattern. The contrast of interference was measured by the thermal imaging camera. In order to collect more light we used cylindrical mirror to produce a line-type image on the thermal viewer. The camera's images are shown on the Fig. 3.

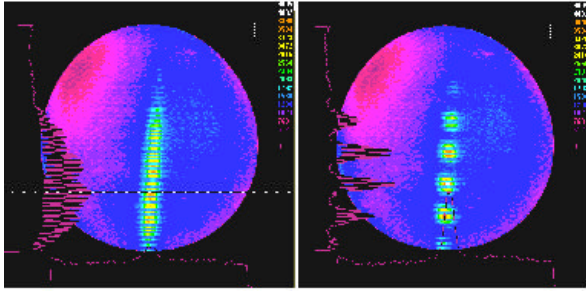


Fig.3. Interference fringes images

The images correspond to the wing of the HGHG pulse (left image, visibility of the fringes is low) and centre of the pulse (right image, visibility is high).

In order to simplify the alignment and tuning of interferometer we used an auxiliary HeNe laser (0.63 μm wavelength) to produce an interference pattern in visible light.

The dependence of visibility $((I_{\text{max}} - I_{\text{min}}) / (I_{\text{max}} + I_{\text{min}}))$ versus delay between two arms for the HGHG pulse measurement is shown in Fig. 4.

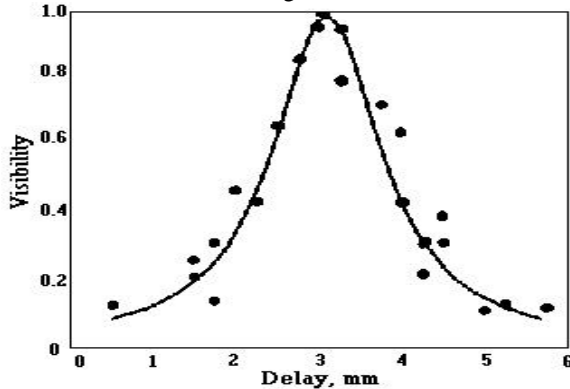


Fig.4. The dependence of visibility versus delay between two arms

The optical coherence length was measured as 1.6 mm, or 5.3 ps, based upon the delay change.

We used an intensity autocorrelator employing a second harmonic generation in AgGaSe₂ nonlinear crystal. The intensity of the second harmonic was measured by a single-element InSb photoconductive detector. The main sources of error in the measurement are imposed by the low-duty cycle (1 shot per 20 seconds) of the CO₂ laser and instabilities in the electron beam. In order to reduce scatter, each data point is a single shot measurement of the second harmonic signal normalized to the square of the fundamental energy. The normalized signal versus delay time (relative length difference between the two arms) is shown in Fig. 5. Assuming a Gaussian pulse shape, the duration is found to be $8.4/\sqrt{2} = 5.9 \pm 0.7$ ps.

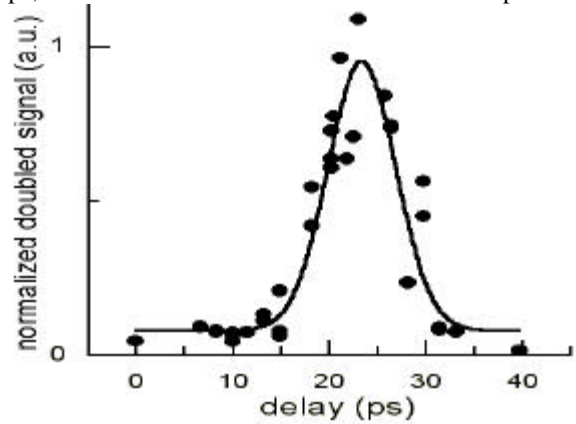


Fig.5. The second harmonic signal versus optical delay

The electron beam energy modulation was determined using the electron energy spectrometer after the radiator section. Energy modulation of the electron beam is generated in two ways in the HGHG process: through the initial interaction of the seed laser in the modulator as well as through the HGHG FEL interaction itself in the radiator. The energy modulation in the radiator predominates and the electron beam image after the spectrometer (a) without and (b) with the CO₂ beam present, is shown in Figure 6. The latter shows an energy modulation of nearly 2.5% FWHM.

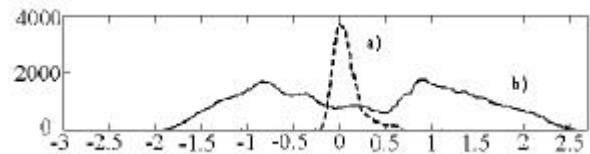


Fig.6. The energy modulation (electron beam distribution after spectrometer, horizontal axis in % of energy spread)

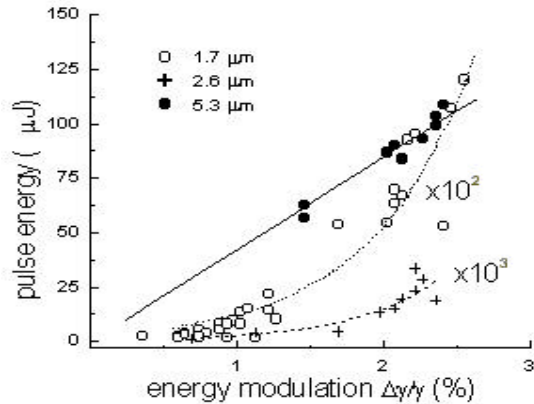


Fig.7. The harmonic power versus FWHM modulation

The amount of modulation, as well as the existence of the higher harmonics, reveals that saturation or near-saturation has been reached. The higher harmonics have been previously predicted in theory [3]. We measured the fundamental (5.3 μm), second (2.65 μm), and third (1.77

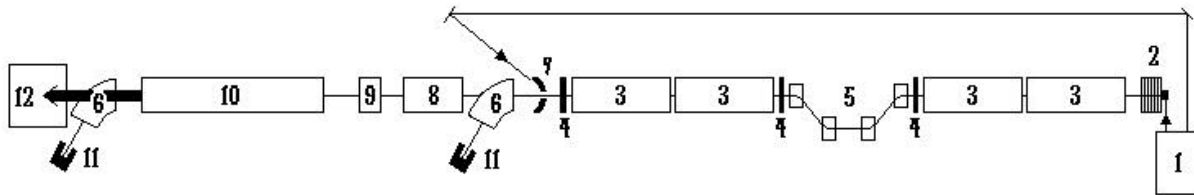


Fig 8. The layout of SDL. 1 – RF gun and seed laser system, 2 – RF gun, 3 – linac tanks, 4 – focusing triplets, 5 – magnetic chicane, 6 – spectrometers dipoles, 7 – axicon mirror, 8 – Mini-undulator, 9 – dispersive section, 10 – NISUS wiggler, 11 – beam dumps, 12 – FEL radiation measurements area.

3. THE DUVFEL PROJECT

The Deep Ultra Violet Free Electron Laser (DUVFEL) in Source Development Laboratory (SDL) [4] is the next step in the development of a short wavelength HGHH FEL. The research plan of DUVFEL includes three stages to generate a coherent radiation of 400 nm, 200 nm and, after energy upgrade, 100 nm coherent radiation.

The layout of the facility is shown in Fig. 8. The accelerator consists of BNL/SLAC/UCLA type electron gun driven by Ti:Sa laser, four SLAC-type linac tanks and a four magnet chicane. A 4.3 MeV electron beam leaves the gun, accelerates up to 60 MeV in two linac sections and compresses in a magnetic chicane. Final acceleration up to 140 MeV is achieved in the last two linac sections.

Last year the commissioning of the SDL accelerator was performed. The RF gun currently can produce 2 ps (RMS) bunches with 300 pC of charge. 4π mm-mrad emittances are measured after acceleration up to 75 MeV in the first two linac tanks. After compression we obtained a 0.3 ps long bunch with the same transverse emittances and 300 amperes peak current.

μm) harmonics as a function of modulation described above using the InSb detector in conjunction with the appropriate band-pass and neutral density filters to produce similar signal levels on the detector.

In Figure 7, the harmonic power (μJ) versus electron beam energy modulation (%) is shown. In Table 2, the theoretical and experimentally measured harmonics to fundamental ratios are shown. There is a good agreement between experiment and theory.

Table 2.

Wavelength	Simulation	Experiment
2.65 μm	6×10^{-4}	2×10^{-4}
1.77 μm	1×10^{-2}	8×10^{-3}

The FEL magnetic system consists of Mini-undulator, dispersive section and 10 m long NISUS undulator [5]. During the first stage of the experiments (400 nm) the harmonic of the Ti:Sa laser will be used as a seed for the HGHH experiment. In order to introduce seed radiation to the vacuum chamber, we discussed two schemes: “small” four magnet chicane, which “bends” the electron beam trajectory around the laser mirror, and a axicon mirror [6]. The last solution is more attractive because of the reduced space requirements and the simplification of electron beam optics.

For electron beam and radiation diagnostics in the NISUS we are going to use 16 pop-in monitors with YAG screens and OTR mirrors. Five of them will be used for FEL radiation measurements, the other five will have shadow shields for OTR measurement to block the spontaneous radiation. The optical spectrometer is installed at the end of the wiggler for the spectrum measurements.

4. REFERENCES

- [1] L. H. Yu, Phys. Rev. A, **44**, 5178 (1991)
- [2] L. H. Yu et al., Science, 289 (2000)
- [3] S.G. Biedron, H.P. Freund, X.J. Wang, and L.-H. Yu, “Nonlinear Harmonics in the High-Gain Harmonic

Generation (HGHG) Experiment”, Proceedings of the 22nd Annual Free-Electron Laser Conference, Durham, North Carolina, August 13-18, 2000.

[4] L. H. Yu et al., “The DUV-FEL Development Program”, these proceedings

[5] D.C. Quimby et al, “Development of a 10-meter Wedged-pole undulator”, NIM A 285 (1989), pp.281-289.

[6] I.V. Pogorelsky and W.D. Kimura, “Waveguiding by axicon focused laser beams”, Adv. Accel. Concepts 1994, pp.419-428